Journal of Archaeological Science 169 (2024) 106025

Contents lists available at ScienceDirect

Journal of Archaeological Science

journal homepage: www.elsevier.com/locate/jas

Revealing primary forming techniques in wheel-made ceramics with X-ray microCT

Ilaria Caloi [a], Federico Bernardini [a,b,*]

[a] Department of Humanities, Ca' Foscari University Venice, Dorsoduro 3484/D, 30123, Venezia, Italy
[b] Multidisciplinary Laboratory, The Abdus Salam International Centre for Theoretical Physics, Strada Costiera 11, 34014, Trieste, Italy

ARTICLE INFO

Keywords:
Ceramic technology
Primary forming techniques
X-ray microCT
Potter's wheel
Experimental archaeology

ABSTRACT

The identification of ceramic forming techniques poses challenges, particularly when different primary and secondary forming techniques are combined, or when specific surface treatments obscure potential diagnostic features. As emphasized in the existing literature, a comprehensive approach should consider all potential sources of information. In this study, we employed a combination of macroscopic observations and X-ray microCT analysis on experimental cups reproduced using the complex technology attested in Middle Bronze Age Crete, i.e. a combination of hand-building technique and potter's wheel. Our investigation focuses on the potential of microCT scanning in unveiling forming techniques in wheel-thrown and wheel-fashioned ceramics. Our results indicate that integrating the visualization of 3D thickness variation in vessel walls, quantification of 2D wall thickness distribution in longitudinal virtual slices, identification of possible structural joints in virtual sections, and evaluation of voids orientation with traditional macroscopic analysis generally allows for the recognition of primary forming techniques and the reconstruction of complex ceramic technological processes.

1. Introduction

In antiquity the potter's wheel could be used in different ways. It could be employed to produce vases directly and entirely, implying that the device's rotative kinetic energy (RKE) was used in the manufacturing process from the very start of each vessel (Courty and Roux, 1995; Roux and Courty, 1998; Roux, 2017, 2019). This is the case of the wheel-throwing and the throwing-off-the hump techniques. Alternatively, it could be used only in a second stage of the manufacturing process, when the rough-out of the vessel body had already been formed through hand-building (Roux and Courty, 1998). Among the hand-building forming techniques, the most common are coil-building, slab-building, layer-building, pinching, molding, and beating (Betancourt, 1979; Todaro, 2016; Thér, 2020 and references there).

The combination of hand-building and potter's wheel has been the focus of many studies in Southern Levant (Roux and Courty, 1998), Mesopotamia (Baldi and Roux 2016) and in the Aegean (Choleva, 2012; Jeffra, 2013), where the potter's wheel was mainly used in combination with coil-building (namely the wheel-coiling technique). Recent studies have also shown that the potter's wheel can be also matched with other hand-building techniques (Todaro, 2016, 2018; Caloi, 2021).

When studying wheel-made vases, whether produced directly on the potter' wheel (i.e. wheel-thrown) or with the help of the potter's wheel (i.e. wheel-shaped or wheel-fashioned), the main concern is to understand the primary forming technique adopted. The potter's wheel can indeed cover over and obliterate the surface traces imparted by the primary forming technique (Van der Leeuw, 1976, 123; Courty and Roux, 1995; Roux, 2019). This means that macroscopic analysis alone is not sufficient to identify the primary forming technique adopted to produce a wheel-made vase.

An innovative use of X-radiography was carried out in the 1970s, when Rye (1977, 1981) first applied it to identify primary forming techniques of vessels. Each ceramic forming technique can produce a characteristic alignment of inclusions and orientation of voids (Rye, 1977). The X-radiography technology was then updated (Berg, 2008) and has successfully been employed by many scholars (see Berg and Ambers, 2017, with references in there). However, this technique has intrinsic limitations, and its effectiveness in pottery studies has also been questioned (e.g. Arnold and Bourriau, 1993, 33–34; Takenouchi and Yamahana, 2021). Radiography, despite its widespread use in archaeological and material science studies, possesses inherent drawbacks

* Corresponding author. Venice Centre for Digital and Public Humanities, Department of Humanities, Ca' Foscari University Venice, Dorsoduro 3484/D, 30123 Venezia, Italy.
E-mail addresses: icaloi@unive.it (I. Caloi), federico.bernardini@unive.it (F. Bernardini).

https://doi.org/10.1016/j.jas.2024.106025
Received 9 April 2024; Received in revised form 7 June 2024; Accepted 9 July 2024
Available online 24 July 2024

when compared to the capabilities of X-ray 3D techniques, such as X-ray computed microtomography (hereafter microCT). Conventional radiography primarily provides a two-dimensional view of an object, offering a single-plane perspective that often fails to capture the intricate details and internal structure comprehensively. This limitation restricts the depth of analysis and may obscure crucial features hidden within the object being studied. Additionally, 2D radiography may encounter challenges in distinguishing overlapping structures or differentiating materials with similar densities, leading to ambiguity and potential misinterpretation of results. These shortcomings underscore the need for a more sophisticated imaging approach to overcome the failings of traditional radiography and facilitate a deeper 3D understanding of archaeological artefacts and materials. This is where microCT, with its ability to generate high-resolution 3D models of the sample microstructure, emerges as an effective technology in the field of imaging and analysis of archaeological materials (Tuniz and Zanini, 2014; Bernardini et al., 2019a; Thér, 2020; Gait et al., 2022).

MicroCT has significantly advanced our ability to reconstruct pottery forming techniques. It enables the 3D visualization and quantification of paste components, including lithic particles, voids, and joints. However, microCT has predominantly been applied to date to prehistoric hand-made ceramics (e.g. Kahl and Ramminger, 2012; Kozatsas et al., 2018; Bernardini et al., 2019b, 2020; Gait et al., 2022). Its potential in reconstructing wheel-throwing technology and the complex building processes of vessels, which combine primary hand-made techniques with potter's wheel use, remains still almost unexplored (Takenouchi and Yamahana, 2021; Thér and Mangel, 2024).

This paper presents, for the first time, the application of microCT to experimental vases, created either solely on the potter's wheel or through a combination of hand-building techniques and potter's wheel. The aim is to assess the capability of microCT in reconstructing complex ceramic technological processes, offering a methodology applicable to the analysis of ancient pottery technology.

2. Materials and methods

2.1. The experimental work

The case study is represented by the analysis of replicas that reproduce wheel-made Minoan cups. The chosen type is a handleless conical cup, attested in the M(iddle) M(inoan) IIA (18th cent. BC) at the archaeological site of Phaistos (Crete), where it was locally produced using different forming techniques, ranging from wheel-throwing techniques (i.e. throwing-off-the-hump and from a solid clay ball) to a combination of techniques that associate a variety of hand-building techniques with the use of the potter's wheel (e.g. wheel-coiling and wheel-pinching). There are two main reasons for choosing this vessel: first, the hundreds of MM IIA handleless conical cups retrieved from structured deposits at Phaistos testify to the contemporary use of different techniques to produce them (Caloi 2012); second, these common cups were manufactured without being given a perfect finish, allowing for an easier identification of macroscopical traces left by the adopted primary forming technique.

2.1.1. Use of Minoan and Minoan-type raw materials, tools, and devices

The experimental work was undertaken by I. Caloi using materials and tools employed in Minoan times, revealed through the archaeological evidence from palatial Crete. She used natural clays collected from Southern Crete clay sources, which are compatible with those used in Early and Middle Bronze Age Crete to produce plain and decorated pottery (Day et al., 2006; Mentesana et al., 2016). Two different clays were used: the first one was grey, the second one was a colluvial *terra rossa* (Mentesana et al., 2016, 305–306). The clay was mixed only with water without any tempering because most conical cups from Phaistos are produced in a very fine and pure fabric, which does not show any lithic temper, just the natural inclusions of the clay. The potter's wheel adopted for experimental replicas was constructed by the potter V. Politakis on the basis of the model proposed by scholars for Minoan Crete (Evely, 1988, Fig. 10; Evely, 2000, 270; Evely and Morrison, 2010).[1] The tools used to trim rims and to apply water to the experimental vases on the wheel were respectively a bronze tool and a natural sponge, while the strand used to cut off the vases from the wheel surface was made from six hairs of a donkey. The vases were fired at 720–800 degrees C in a pit-kiln (Caloi, 2019, Fig. 5), reconstructed by Politakis following the Minoan pit-kilns found at Phaistos (e.g. Todaro, 2009, p. 337, Fig. 2).

2.1.2. The experimental reproduction of four forming techniques

Four groups of experimental handleless conical cups were produced by the potter V. Politakis using four ceramic techniques, making a total of 60 replicas (see Table 1).

Group 1 includes 25 replicas produced using the throwing-off-the-hump technique (Fig. 1a–b). That is fashioning small vases from the clay at the top of a large lump, called also a mound. Placing the mound on the wheel as one piece, it was centred, starting from the top. The clay was pressed down against the wheel head as it was centred. The second step was opening up the very top of the mound and pulling the clay up to make the cup. Finally, the cup was cut off the hump with the strands of hair.

Group 2 is composed of 15 replicas produced on the potter's wheel throwing from a solid ball of clay (Fig. 1c–d). The clay ball was placed on the potter's wheel, then pressed with the thumbs in order to centre it. The clay was then pulled up to make the cup, which was finally cut off from the potter's wheel using the strands of hair.

Group 3 includes 10 replicas produced using the wheel-pinching technique, that is the formation of a handleless cup from a small clay ball (i.e. pinching) and then the final shaping of this cup on the wheel (Fig. 1e–f). For this experiment, the general outline for the pinching technique was followed (Rice, 1987, 125–126). First the clay was made into a lump, then a hole was pushed into it by pressing a thumb into the centre, while supporting the outside with the fingers. Then, the walls were progressively thinned by pressing and squeezing the clay between the thumb and the fingers. When the rough-out was ready, it was put on the wheel to thin the walls and fashion the final form.

Group 4 includes 10 replicas produced using the wheel-coiling, i.e. a technique involving first the coil-building of a cup and then its final shaping on the wheel. For 9 replicas, three coils of 1 cm thickness were used and then set on a circular base 1 cm thick and 3 cm across. Only one replica (5CW) was produced using five coils set on a circular base. The joints between the coils were oriented towards the interior, to match the traces of coils left on the archaeological material from MM IIA deposits of Phaistos. Once the coils were positioned, the wheel was exploited for joining the coils, thinning the walls, and shaping the roughout (Fig. 1g–h). Once the roughing-out was achieved, the pot was finally shaped on both its upper and lower parts on the wheel. The surfaces

Table 1
Experimental reproductions with the indication of those analysed by microCT.

Groups	Forming techniques	N. of replicas	Analysed replicas
Group 1	Throwing-off-the-hump	25	H3, H14, H21
Group 2	Wheel-throwing from a solid ball of clay	15	SB3, SB4, SB5
Group 3	Wheel-pinching	10	PN2, PN3, PN7
Group 4	Wheel-coiling	10	3C2, 3C5, 5CW

[1] For a description of how the experimental potter's wheel was constructed and used by V. Politakis see: Caloi (2021).

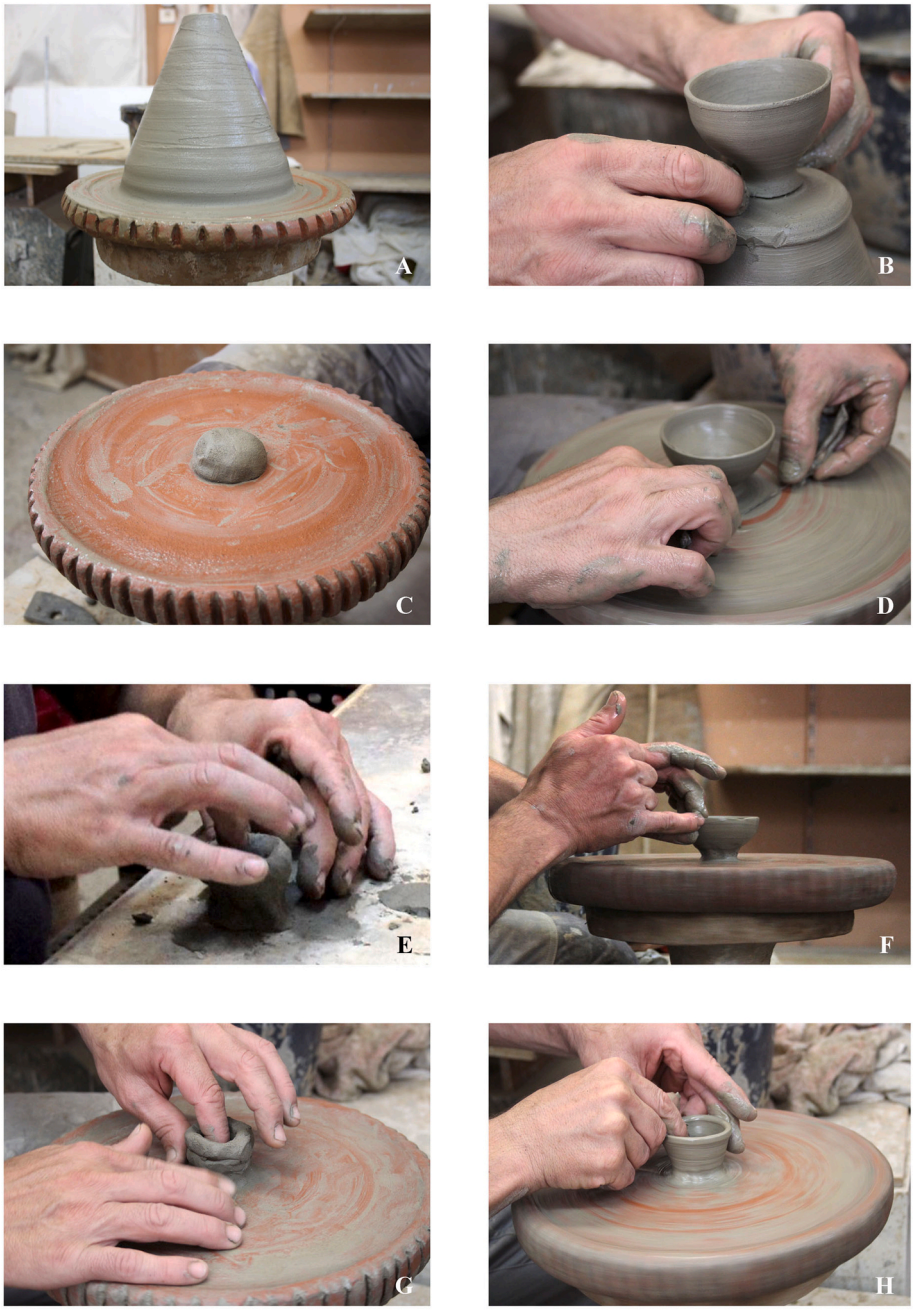

Fig. 1. a–b: the lump or mound of clay (a) and the handleless cup cut-off-the-hump (b); c–d: the wheel-throwing technique from a solid clay ball: the clay ball on the potter's wheel (c) and the produced cup, cut-off the potter's wheel using a strand (d); e–f: the wheel-pinching technique: the rough-out of the pinched cup and the final shaping of the cup on the potter's wheel (f); g–h: the wheel-coiling technique: the cup is coil-built on the potter's wheel using three coils on a circular base (g) and then shaped on the device (h).

were left as they were, without smoothing them. This technique corresponds to the wheel-coiling Method 3, first defined by V. Roux and Courty (1998) for Southern Levant, and then recognized by C. Jeffra (2013) in Minoan ceramics.

2.2. X-ray computed microtomography

12 cups (3 from each group) have been analysed by microCT (Table 1) at the Multidisciplinary Laboratory of the Abdus Salam International Centre for Theoretical Physics, using a system (Tuniz et al., 2013) specifically designed for the study of archaeological and paleoanthropological samples (e.g. Bernardini et al., 2016, 2019b; Di Vincenzo et al., 2017; Tuniz et al., 2012; Zanolli et al., 2018). The microCT scans were carried out by using a sealed X-ray source (Hamamatsu L8121–03) with a focal spot size of 5 μm and a flat panel detector (Hamamatsu C7942SK-25; pixel size of 50 μm) according to the following parameters: 110 kV, 90 μA, exposure time/projection of 2 s, 1440 projections of the samples over 360°. The X-ray beam was filtered by a 0.01 mm-thick copper absorber. The final slices were reconstructed using the commercial software DigiXCT (Digisens) in 32-bit format at an isotropic voxel size of 40 μm.

2.2.1. Image processing

MicroCT virtual reconstructions have been used to visualize the thickness variation of pottery walls, to identify potential structural joints resulting from the primary forming techniques and to virtually extract

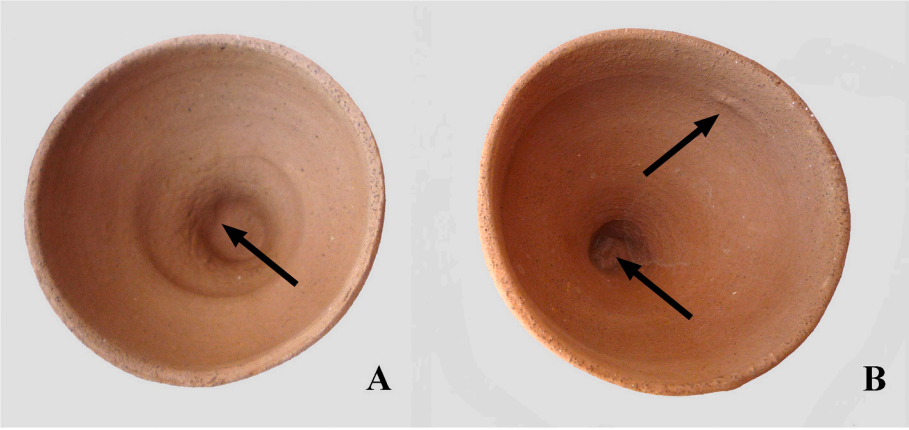

Fig. 2. Group 1 (Wheel-thrown-off-the-hump replicas). Narrow and deep hollow with clay bumps (a) and clay barb-like protrusions (b).

the pores for visualizing their orientation.

2.2.1.1. Thickness variation of pottery walls

2.2.1.1.1. 3D thickness distribution. Thickness maps of the walls of the investigated cups have been produced using Avizo v.8 (Visualization Sciences Group Inc.). Within the segmentation editor panel ("Edit New Label Field"), we separated the air (labeled "exterior") and the walls of the vessels (labeled "walls"), while assigning the base and the rim of the cups to a different material. The space between this material and the inner surface of the walls was segmented (labeled "interior"). The 3D surfaces were reconstructed with unconstrained smoothing. The interfaces between the "walls" and the "interior", as well as between the "walls" and the "exterior", were extracted using the "Surface View" panel. Subsequently, thickness maps were generated by computing the distance between these two surfaces via the "Surface Distance" panel.

2.2.1.1.2. 2D thickness distribution in longitudinal central sections. Longitudinal virtual sections passing through the centre of the vessels were generated using Avizo v.8 (Visualization Sciences Group Inc.). The 2D wall thickness distribution was measured from the rim to the base every 500 μm using the free software package MPSAK v.2.9 (Dean and Wood, 2003; see Fig. S1). Two sections per sample were measured.

We decided to focus on longitudinal central sections based on the visualization of the 3D thickness distribution (see below), which indicated a significant thickness variation along the longitudinal plane of the investigated vessels. Additionally, a recent quantitative evaluation of thickness variability in selected horizontal slices (Thér and Wilczek, 2022) has not provided conclusive results.

2.2.1.2. Virtual sections and technological joints. The entire datasets have been thoroughly examined through virtual cross-sectioning. Transversal and longitudinal sections have been produced by Avizo v.8 (Visualization Sciences Group Inc.) and VGStudio Max v.2.0, identifying primary structural joints whenever possible.

2.2.1.3. Visualization of voids orientation. The alignment and orientation of both voids and lithic particles can provide information about pottery forming techniques (Berg, 2009, 2011; Thér, 2020 and references there). However, the segmentation of voids is generally a much faster process, especially when the X-ray attenuation coefficient of lithic grains is not significantly different from that of the clayey components. For this reason, we have focused our analysis on void orientation.

Using Avizo v.8 (Visualization Sciences Group Inc.) and with the limitations given by the voxel size, a semi-automatic threshold-based segmentation has been carried out in order to separate the voids from the pottery body. To achieve such target, the half-maximum height protocol (HMH) has been adopted (Fajardo et al., 2002; Coleman and Colbert, 2007). This method, developed mainly for bone materials, calculates the threshold value as the mean of the minimum and maximum grey scale values along a row of pixels crossing the pores to paste transition. The mean value of 10 HMH values, calculated for the same number of slices randomly selected, has been taken as threshold for the complete datasets. In some cases, the threshold values have been visually adjusted until threshold limits corresponded to pores boundaries. This operation has been repeated many times applying different thresholds until voids have been correctly separated. The 3D surfaces were reconstructed with no smoothing.

To qualitatively assess the orientation of the voids, we generated comparative images of the different technological Groups 1–4 (Figs. 9–12, S6-13). These images include a shaded rendering of the vessels, a representation of the voids combined with the vessel surface in transparency, an image similar to the last one but with a longitudinal central slice as a background, and an interpretation of void orientation overlaid on the last image. The purpose of including a slice as a background in one of the selected images is to visualize only the pores present in half of the vessel, making it easier to discern their orientation. In the simple rendering with shaded pores and the vessel in transparency, the pores on both the front and back walls are overlapped, making their orientation difficult to assess (Figs. 9–12, S6-13).

3. Results

3.1. Macroscopic analysis of replicas

The macroscopic analysis of replicas has shown that there are some features that seem to be attributable to a single primary forming technique, whereas there are others that seem random and cannot be accepted as clear evidence of a specific forming technique, like the striations on the base exterior (see Courty and Roux 1995; Roux 2019, 178–180).

3.1.1. Group 1 (wheel-thrown-off-the-hump replicas)

There are some clusters of features that seem to characterise the wheel-thrown-off-the-hump vases, like a deep but narrow hollow on the interior of the vase, associated with clay lumps and bumps (Fig. 2a–b) and clay barb-like protrusions (Fig. 2b). Unlike the shallow hollow attested on some wheel-pinched and wheel-coiled experimental cups, that on the wheel-thrown ones is usually deep (0.5 cm), narrow (0.5–1.5 cm), and of a conical section. This feature is likely due to the strong, initial pressure that is necessary to apply in order to centre the large mound of clay on the potter's wheel. It is often associated with evidence of wet clay, such as sticky fingerprints or wrinkles. This macroscopic feature, which so far cannot be considered univocal, has been however observed also by Doherty on the wheel-thrown miniatures vases from Naqada in Egypt (Doherty, 2015, 2021).

The abovementioned evidence of exceptionally wet clay, the barb-like protrusions and/or sticky fingerprints (Fig. 2), could reflect the fact that the throwing-off-the-hump technique requires the clay to be kept continuously wet. In comparison to the other technique employing RKE, the large lump of clay used to throw cups needs a major amount of water during the manufacturing process.

The decreasing thickness from the base to the rim appears especially on wheel-thrown cups of Group 1 and 2. The thickness of the rim is uniform and constant, and ranges from 2 to 3 mm.

3.1.2. Group 2 (wheel-thrown replicas from a solid clay ball)

The wheel-thrown replicas from a solid clay ball do not show specific features, which by themselves can be interpreted as diagnostic of this technique. They often show a step between the base and the upper body of the vessel (Fig. 3a–b), which internally corresponds to the above-mentioned hollow. This, however, is not recurrently deep and narrow as in the wheel-thrown cups of Group 1. As in specimens of Group 1, some wet clay in the shape of wrinkles or clay bumps is visible in the interior walls (Fig. 3b).

As already said, the regularity in the wall and rim thickness is a feature observed only in wheel-thrown cups, of both Group 1 and 2.

3.1.3. Group 3 (wheel-pinched replicas)

For this particular experiment, wheel-pinched vases have strong finger imprints on the outer face, especially on the lower part of the vase (Fig. 4b), which are associated with horizontal rilling on the upper part (inside and/or outside). The outer face may also show crevices in association with the hollows left by the finger imprints. The inner face frequently presents a smooth surface or may show fingerprints and/or short lines near the rim left by the potter's finger (Fig. 4a). The thickness of the walls is very irregular and does not necessarily change from the base to the rim, as observed on the wheel-thrown cups (Groups 1–2). Moreover, the rim thickness is not uniform along the circumference of the vase rim, ranging from 2 to 4 mm.

3.1.4. Group 4 (wheel-coiled replicas)

There are some features that seem attested only on wheel-coiled replicas, like short horizontal or curvilinear fissures, which appear both on the inner and outer face (Fig. 5a–b) and are often associated with compression folds (Fig. 5b). On some wheel-coiled replicas, the inner face has horizontal lines indicating the imperfect joining of the coils (Fig. 5b). Wheel-pinched and wheel-thrown vessels do not show any similar fissures.

Most wheel-coiled replicas have an irregular thickness to the walls, which do not gradually decrease from the base to the rim as in the specimens of Groups 1 and 2. Likewise, the rim thickness is not uniform and regular along the circumference of the vase rim.

There are also wheel-coiled replicas that do not show specific features whatsoever, likely due to the fact that the coils have been perfectly joined. As already said, the final shaping of vases can cover up any and all traces imparted during the primary forming technique.

3.2. X-ray microCT results

3.2.1. Thickness variation of pottery walls

3D thickness maps reveal differences between thrown-off-the-hump cups (Group 1), cups produced using the wheel-throwing technique from a small clay ball (Group 2), and other wheel-pinched and wheel-coiled cups (Groups 3 and 4, respectively; Fig. 6; Figs. S2–5).

The first two groups exhibit a similar thickness distribution, characterised by a thickness increase noticeable at about 1.5 cm from the base, followed by very homogeneous horizontal bands, with the thickness gradually decreasing towards the rim (Figs. S2–3). In contrast, both Groups 3 and 4 display irregular thickness related to the primary forming techniques (Figs. S4–5).

The 2D quantification of wall thickness in longitudinal central sections (Table S1, Fig. 7) aligns with the evidence provided by 3D thickness maps. The thickness profiles of Groups 1 and 2 are characterised by an increased thickness at about 1.5 cm from the base (up to 6–7 mm), followed by a regular and gradual decrease towards the rims, which have a consistent thickness of approximately 2–3 mm.

The profiles of the vessels in Groups 3 and 4 show much higher variability and different patterns. The wheel-pinching vessels of Group 3 display quite irregular decreasing profiles in vessels PN3 and PN7, while vessel PN2 shows an increasing trend from the centre of the vessel to the rim. The rim thickness varies from about 2 to 4 mm. The wheel-coiling vessels of Group 4 exhibit various profiles, with thickness either decreasing (vessel 3C2), increasing (vessel 5CW) or remaining quite constant (vessel 3C5) from the base to the rim. The rim thickness varies between 1.5 and 3.5 mm.

3.2.2. Virtual sections and primary structural joints

The capability to virtually section the microCT models facilitates the examination of potential joints arising from the primary production techniques of the vessels (Kahl and Ramminger, 2012; Sanger et al., 2013; Sanger 2016; Kozatsas et al., 2018; Bernardini et al., 2019a). In this specific case, the persistence of discontinuities typically produced by the coiling technique was confirmed in two vessels (cups 3C2 and 5CW; Fig. 8). Among the three experimental cups analysed that were produced by the coiling technique, the wheel-shaping process eliminated these traces in only one of them (3C5). In the 5CW sample, produced using five coils and a base, sub-horizontal joints are visible just above the base and probably represent the junction between the lowest coil and the bottom of the vessel (Fig. 8). In the 3C2 vessel, produced using three coils on a circular base, sub-horizontal discontinuities likely indicate the joints between the first and second coil and the second and

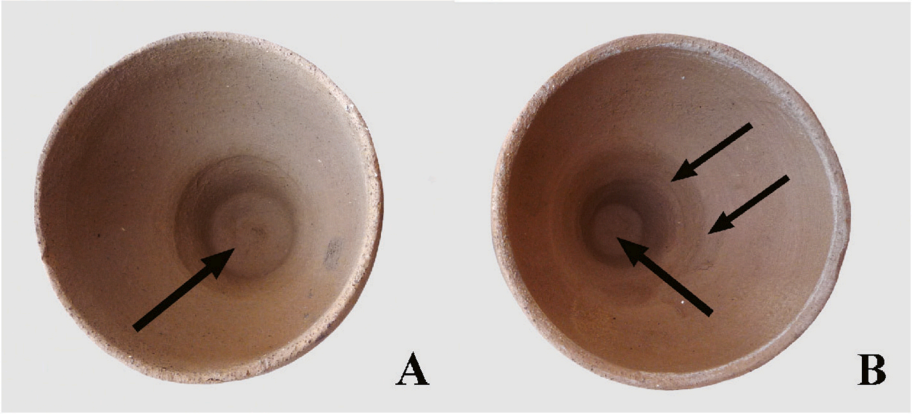

Fig. 3. Group 2 (Wheel-thrown replicas from a solid clay ball). Narrow and deep hollow with a clay bump (a) and wrinkles (b).

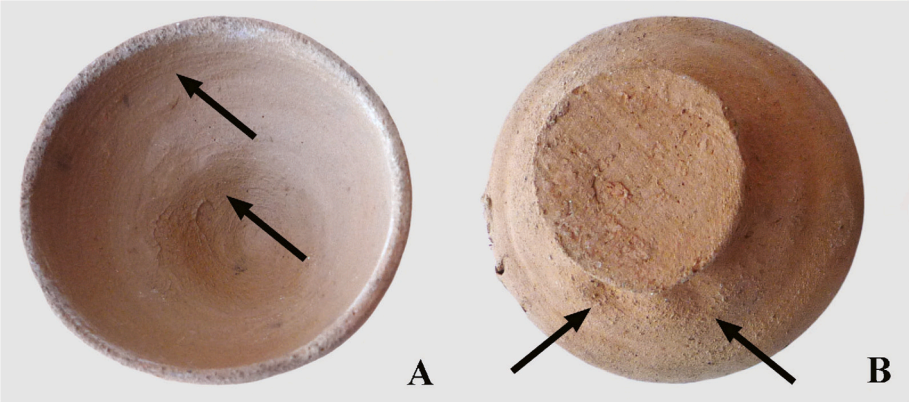

Fig. 4. Group 3 (Wheel-pinched replicas). Horizontal rilling on the upper part and fingerprints (a); hollows and strong finger imprints on the outer face (b).

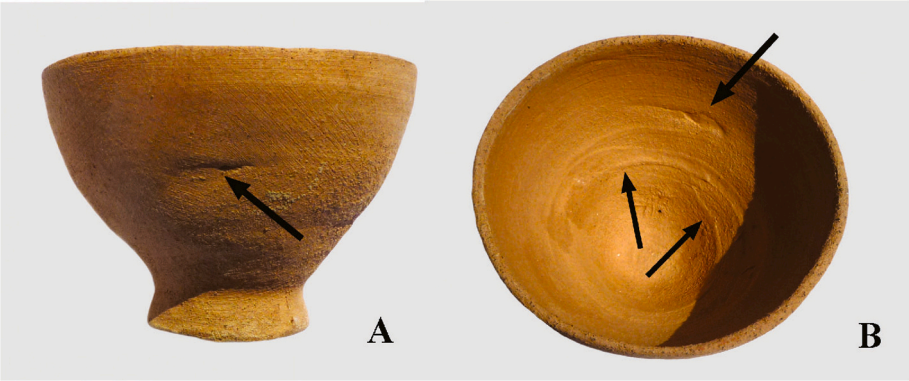

Fig. 5. Group 4 (Wheel-coiled replicas). Horizontal fissures on the external face and in the inner face (a–b); compression folds and horizontal lines in the inner face (b).

third coil (Fig. 8).

No technological joints have been detected in the cups modelled through the pinching technique.

3.2.3. *Void orientation*

In the frontal view (i.e. from the side), vessels of Group 1 exhibit voids with a diagonal orientation, originating almost from the bottom of the cups. When observed perpendicularly to the bottom of the cups (i.e. from the base, looking down), these voids can form a spiral pattern, which is prominently visible in sample H3 (Fig. 9, Fig. 13).

Conversely, in the frontal perspective, vessels within Groups 2 and 3 predominantly display diagonally oriented voids in their central and upper regions, while the distribution at their bases appears either random or less distinctly identifiable (refer to Figs. 10 and 11; Figs. S8–11). For Group 2, this tendency likely arises from the manufacturing process involving a solid clay ball initially pressed at the centre before shaping the cup. Similarly, the wheel-based modification of a pinched vessel (Group 3) predominantly alters the volume and microstructure of the walls, with minimal impact on its base.

Group 4 exhibits voids that, in a frontal view, are horizontally oriented and show a variable density that reflects the position and structure of the original coils used to construct the vessel roughouts before their final shaping on the wheel (Fig. 12; Figs. S12–13). In samples 3C2 and 3C5, the three original coils used to shape the vessels, particularly the second and third ones, remain readily identifiable (Fig. 12; Fig. S12).

Lastly, it is noteworthy that the distinct orientation of voids can sometimes be visible when observing the vessel bases perpendicularly. Unfortunately, all the information is compressed into a single plane, as in radiography, which can lead to an unclear recognition of void patterns compared with their observation from a frontal view with a central longitudinal slice as the background.

As depicted in Fig. 13 and Fig. S14, H3 and H14 of Group 1 showcase a quite clear spiral arrangement of voids. In Groups 2 and 3, this spiral arrangement, when visible, appears less organized, particularly towards the centre of the vessels, where voids lack discernible orientation patterns within the bases (see SB3 and SB4 in Fig. S14). Conversely, in Group 4, the voids apparently adopt a concentric pattern, resembling that of a circular target (Fig. 13 and Fig. S14), quite well recognizable in vessels 3C5 and 5CW.

Such results demonstrate that observing void orientation perpendicular to the bottom of the cups alone cannot securely identify the technological process and must be considered together with other technological indicators.

4. Discussion and conclusions

The identification of ceramic forming techniques becomes challenging when different primary and secondary forming techniques are combined, or when specific surface treatments obscure potential diagnostic features. As extensively highlighted in the literature (references in Thér, 2020), a comprehensive approach should consider all potential sources of information. In this context, the availability of X-ray 3D non-destructive analytical methods, when combined with macroscopic observations, represents a potential game-changer in the study of ancient pottery technology. In this study, we have tested such an approach through the microCT analysis of cups experimentally reproduced according to the combined techniques in use during the Middle Minoan period on Crete (see Knappett, 1999; Berg, 2011; Caloi, 2011, 2019, 2021; Jeffra, 2013).

The obtained results indicate that the observation of surface features,

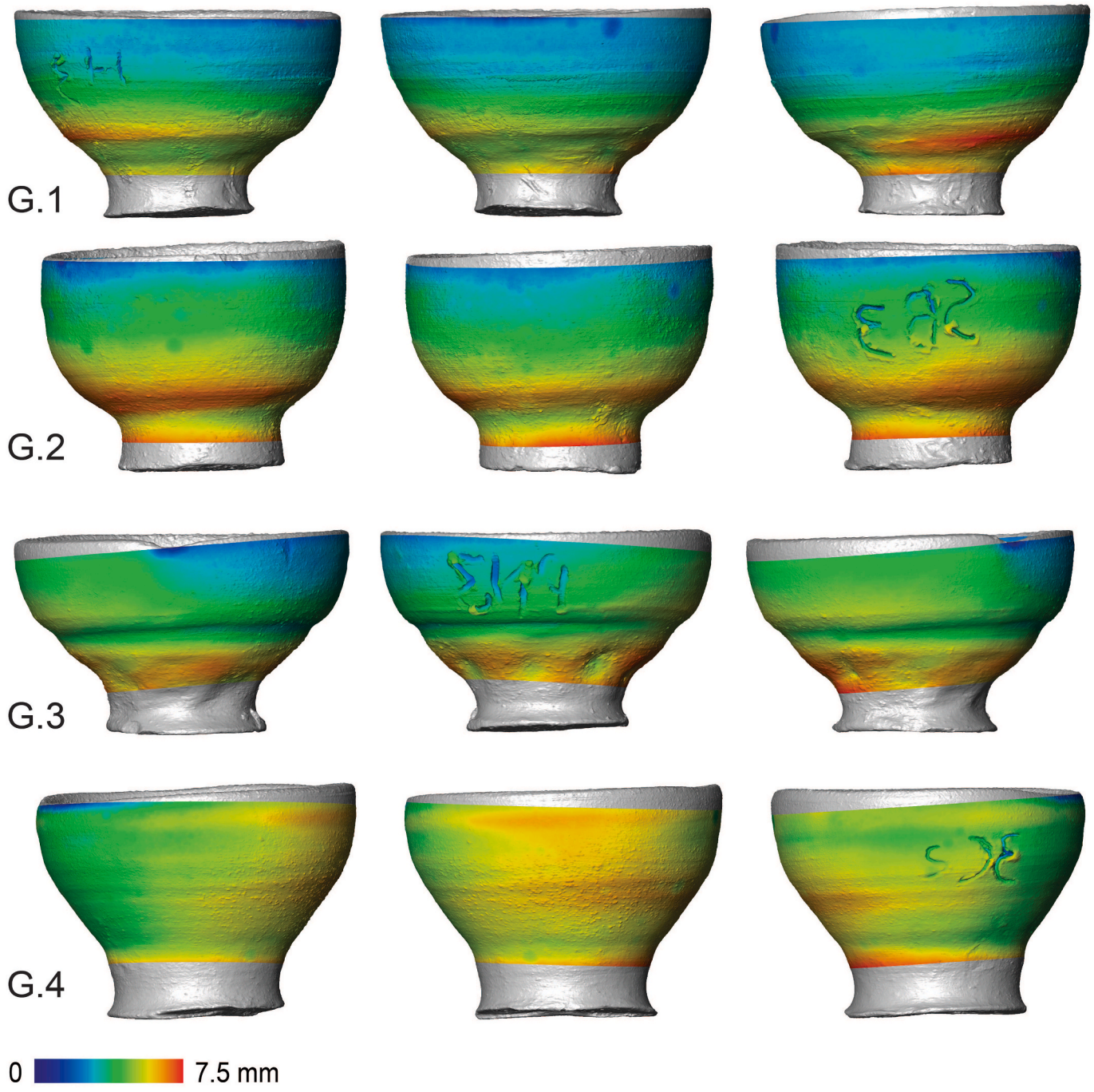

Fig. 6. MicroCT-derived thickness maps of selected cups belonging to Groups 1–4 (G.1-G.4: H3, SB3, PN3 and 3C5, respectively) rendered by a false-colour scale. Image not to scale. For the thickness maps of all analysed samples see Figs. S2–5.

coupled with microCT-derived information – specifically the identification of joints through virtual sectioning, the visualization of 3D and 2D thickness variation of pottery walls, and the orientation of voids – provides combined insights that illuminate technological processes (Table 2). The orientation of particles and voids can be qualitatively assessed or quantitatively defined, although the latter approach has, so far, been implemented only for small volumes (e.g. Gait et al., 2022), not representative of the entire vases.

However, it is important to emphasize that our results confirm the necessity of considering all the aforementioned technological indicators jointly to achieve a confident reconstruction of the technological processes. Major technological joints have been identified only in Group 4 (Fig. 8). Thickness variation, both in 3D visualizations and 2D longitudinal central slices, shows a clear difference between Groups 1–2 and Groups 3–4, with the former characterized by a relatively standardized pattern and the latter showing irregular thickness distribution (Figs. 6 and 7; Figs. S2–5). Such results about thickness variation confirm the results of previous 2D studies, even if carried out using a different methodological approach (Thér and Wilczek, 2022). Our visualization of 3D thickness maps of vessel walls is significant because it provides one of the first attempts to measure thickness variation in 3D and not along a few selected slices of vessels. The orientation of voids from a frontal view ranges from a horizontal direction in Group 4 to a clear diagonal direction in Group 1 (Figs. 9–12; S6-13), with Groups 2 and 3 generally showing a diagonal orientation, except at the base. Observing the voids perpendicularly to the base has generally not

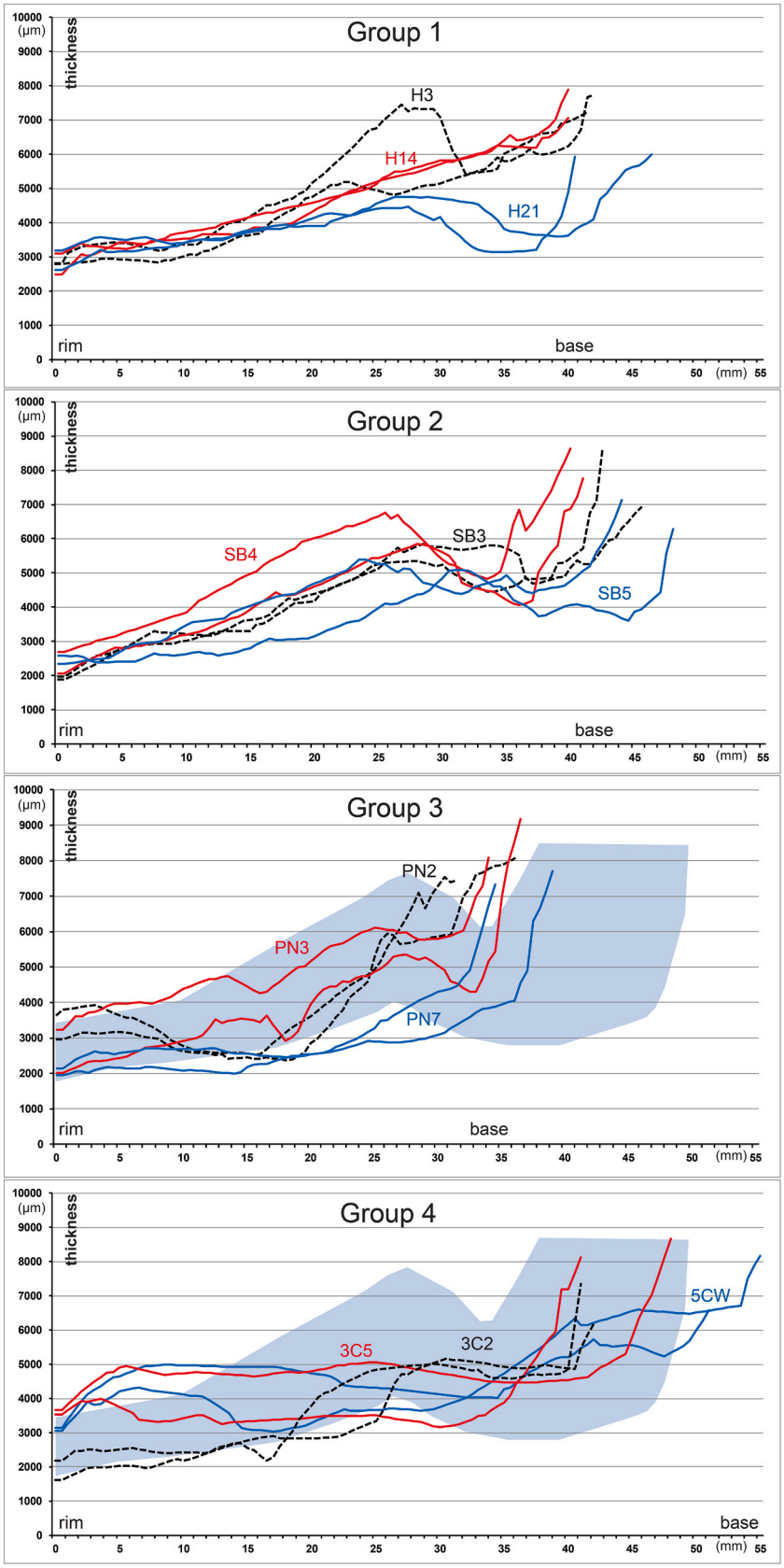

Fig. 7. Wall thickness distribution from rims to bases in 2 longitudinal central sections per sample. The light blue area corresponds to the range of wall thickness distribution for Groups 1–2. For all measurements, see Table S1.

Fig. 8. Virtual sections of wheel-coiled cups 3C2 and 5CW, where primary technological joints are indicated by white arrows. Images not to scale.

provided a clear distinction between groups (Fig. 13 and S14).

Vessels produced through the throwing-off-the hump technique (Group 1) display a distinctive hollow visible to the naked eye on the internal base of the cups (see Fig. 2; see comparisons in Doherty, 2015, 2021). These vessels exhibit a thickness increase noticeable at about 1.5 cm from the base, followed by a gradual and homogeneous decrease towards the rim. Moreover, voids are diagonally oriented from the base to the rim and are arranged in a spiral shape when viewed perpendicularly to the bottom.

Vessels produced using the potter's wheel from a solid clay ball (Group 2) bear similarities to those in Group 1 (Fig. 3). However, the voids seem to be diagonally oriented primarily in the central and uppermost regions of the body, while displaying a random orientation at the base. As a result, a distinct spiral shape is not clearly visible when viewed perpendicularly from the bottom.

Cups modelled using the pinching technique and then shaped on the wheel (wheel-pinching: Group 3) generally exhibit macroscopic irregularities mostly preserved on the external face, close to the base (Fig. 4), an irregular thickness distribution, which distinguish them from those of Group 2, and a void orientation similar to that observed on vessels of Group 2. A distinct spiral shape is not clearly visible when viewed perpendicularly from the bottom.

Cups modelled using the wheel-coiling technique (Group 4) exhibit horizontal lines and/or fissures that are macroscopically visible (Fig. 5) and an irregular thickness distribution. In some cases, bands derived from the original coils still create thickness anomalies, and the pores retain the primary horizontal orientation imparted by the coils. Hence, when observing the vessel bases perpendicularly, a concentric arrangement of voids resembling a target pattern is sometimes recognizable. Furthermore, technological joints can be preserved and detected in virtual sections. All the data indicate that wheel-coiled vessels of Group 4, compared to those of other groups, exhibit the most distinct characteristics, making it relatively easy to recognize their primary technology.

Our study confirms the effectiveness of microCT in overcoming the significant and inherent limitations associated with radiography, particularly the cumulative attenuation of X-rays throughout the entire sample thickness. This attenuation often results in the overlapping of voids and lithic particles in 2D radiographs. In contrast, microCT-

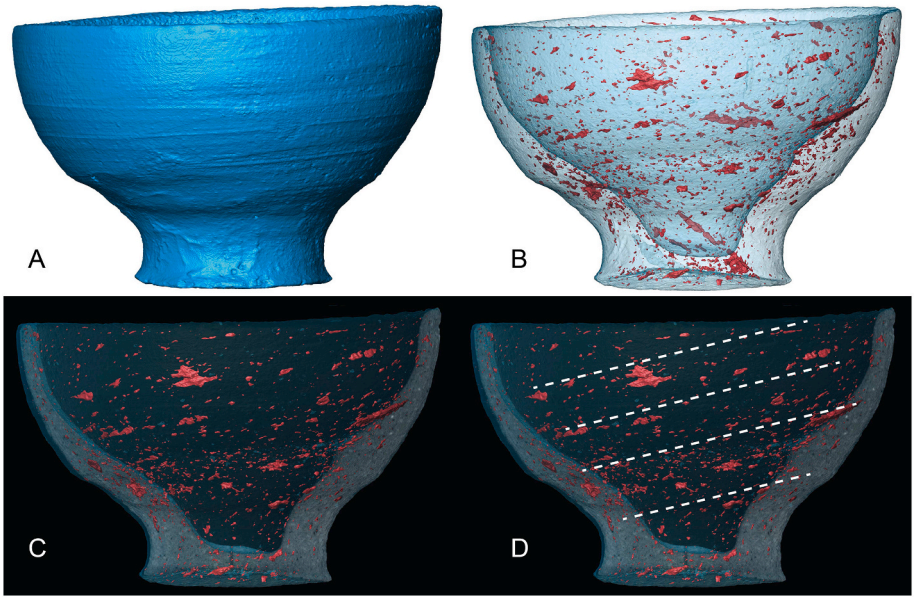

Fig. 9. Orientation of voids in Group 1, cup H3. Image not to scale. A: shaded representation of the vessel; B: transparent paste with voids highlighted in red shading; C: transparent paste with voids highlighted in red and a central longitudinal virtual slice as the background; D: similar to C, with interpretations (dotted white lines indicating void orientation).

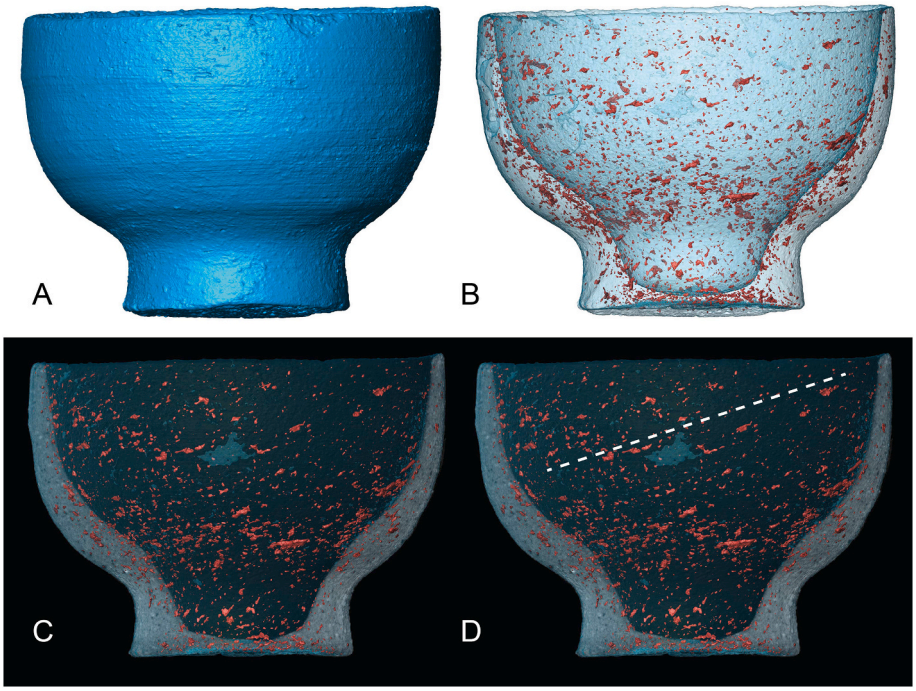

Fig. 10. Orientation of voids in Group 2, cup SB3. Image not to scale. A: shaded representation of the vessel; B: transparent paste with voids highlighted in red shading; C: transparent paste with voids highlighted in red and a central longitudinal virtual slice as the background; D: similar to C, with interpretations (dotted white lines indicating void orientation).

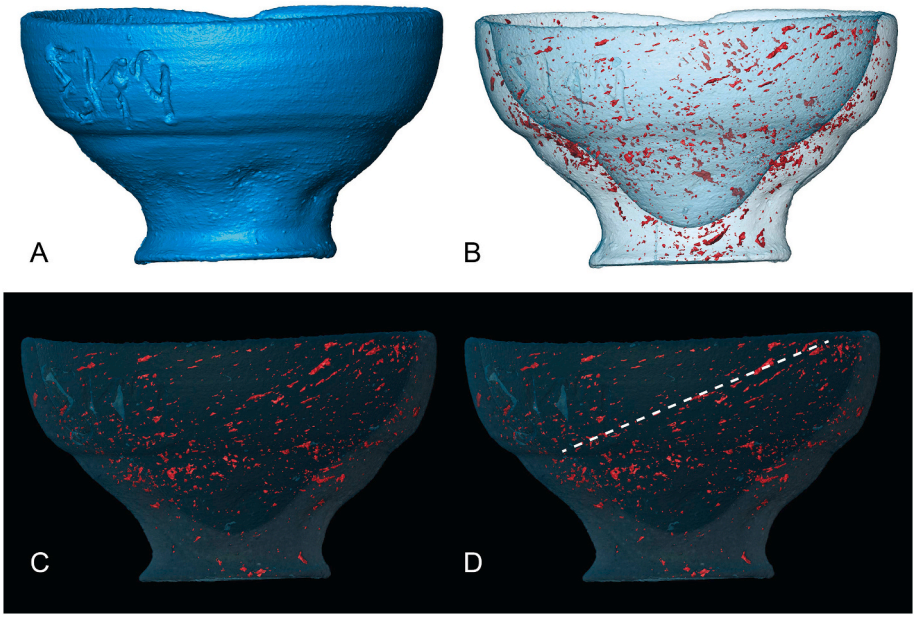

Fig. 11. Orientation of voids in Group 3, cup PN3. Image not to scale. A: shaded representation of the vessel; B: transparent paste with voids highlighted in red shading; C: transparent paste with voids highlighted in red and a central longitudinal virtual slice as the background; D: similar to C, with interpretations (dotted white lines indicating void orientation).

derived virtual models offer the advantage of multidirectional virtual sectioning, segmentation, virtual extraction, and analysis of all primary paste components. However, future research should focus on the development and application of 3D quantification approaches essential for statistically testing the indications provided by the observation of the diagnostic features presented in this paper. Nonetheless, the integration of microCT-derived data with traditional macroscopic observation has revealed discriminative features associated with some of the most common techniques or their combinations. In many cases, this integration enables the identification of primary and secondary forming techniques and facilitates the reconstruction of complex ceramic technological processes when all technological indicators are considered together.

Data availability

MicroCT data are available at https://zenodo.org/records/12743544.

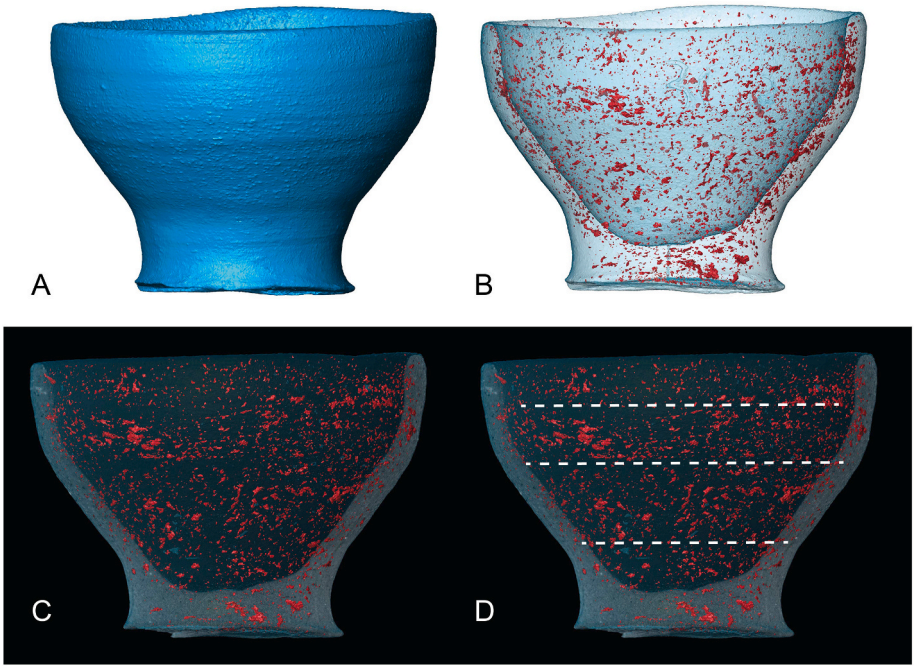

Fig. 12. Orientation of voids in Group 4, cup 3C5. Image not to scale. A: shaded representation of the vessel; B: transparent paste with voids highlighted in red shading; C: transparent paste with voids highlighted in red and a central longitudinal virtual slice as the background; D: similar to C, with interpretations (dotted white lines indicating void orientation).

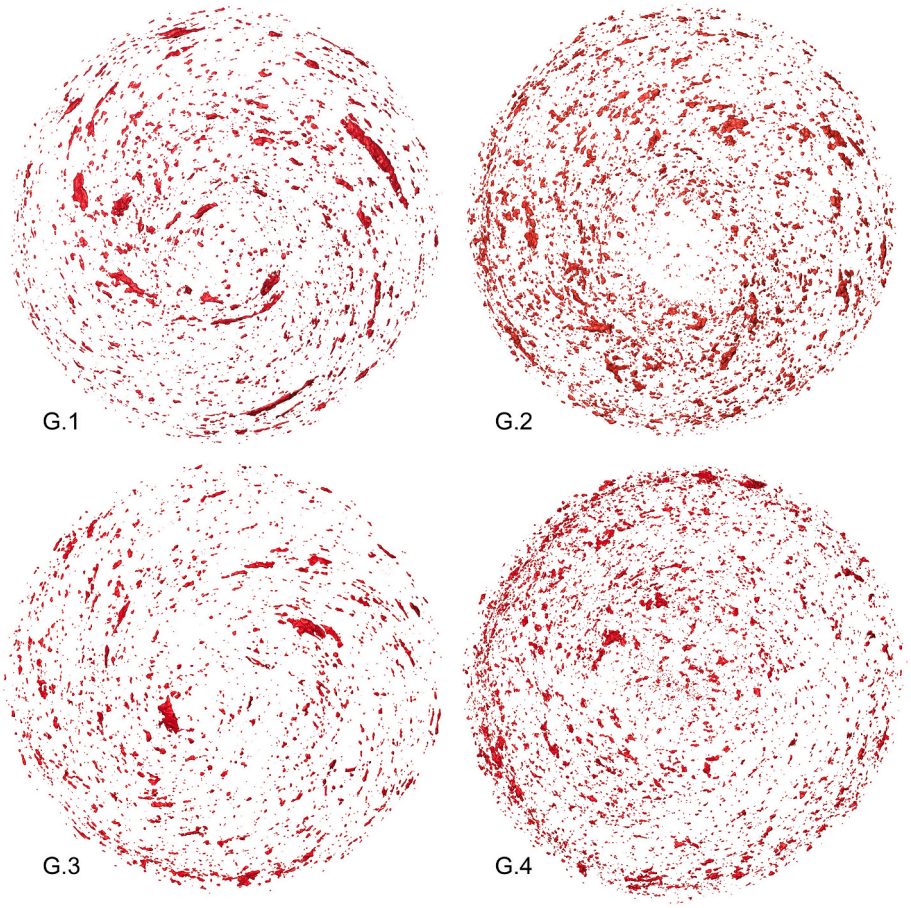

Fig. 13. Voids orientation viewed perpendicular to the base in selected vessels of Groups 1–4 (G.1-G.4: H3, SB3, PN3 and 3C5, respectively). Image not to scale. For images of all analysed vessels see Fig. S14.

Table 2
Main diagnostic features of primary forming techniques in wheel-thrown and wheel-fashioned ceramics.

Groups	Major discontinuities	Thickness variation of walls	Void orientation Frontal view	Void orientation Perpendicular view
Group 1	None	Gradual decreasing towards the rim	Diagonal	Distinct spiral pattern
Group 2	None	Gradual decreasing towards the rim	Diagonal, except the base	Less organized spiral pattern at the centre
Group 3	None	Irregular	Diagonal, except the base	Less organized spiral pattern at the centre
Group 4	External and internal joints	Irregular	Horizontal	Concentric pattern

CRediT authorship contribution statement

Ilaria Caloi: Writing – review & editing, Writing – original draft, Project administration, Methodology, Investigation, Funding acquisition, Conceptualization. **Federico Bernardini:** Writing – review & editing, Writing – original draft, Visualization, Software, Methodology, Investigation, Funding acquisition, Conceptualization.

Ilaria Caloi authored chapters 2.1 and 3.1, while Federico Bernardini authored chapters 2.2 and 3.2. All other chapters were collaboratively written by both authors.

Declaration of competing interest

The authors declare that they have no known competing financial interests or personal relationships that could have appeared to influence the work reported in this paper.

Acknowledgments

We express our gratitude to Don Evely for the English revision of the manuscript, to Alessandro Sanavia for preparing Figs. 1–5, and to Clément Zanolli for providing valuable suggestions regarding the elaboration of microCT datasets. Additionally, we acknowledge the financial support provided by the Venice Centre for Digital and Public Humanities of Ca' Foscari University for our research. We thank the anonymous reviewers for their insightful comments.

Appendix A. Supplementary data

Supplementary data to this article can be found online at https://doi.org/10.1016/j.jas.2024.106025.

References

Arnold, D., Bourriau, J., 1993. An Introduction to Ancient Egyptian Pottery. Verlag Philipp Von Zabern, Main am Rhein.
Baldi, S., Roux, V., 2016. The innovation of potter's wheel: a comparative perspective between Mesopotamia and the southern Levant. Levant 48, 236–253.
Berg, I., 2008. Looking through pots: recent advances in ceramics X-radiography. J. Archaeol. Sci. 35, 1177–1188. https://doi.org/10.1016/j.jas.2007.08.006.
Berg, I., 2009. X-radiography of knossian bronze Age vessels: assessing our knowledge of primary forming techniques. BSA 104, 137–173.
Berg, I., 2011. What's in a forming technique? An investigation into wheel-throwing and wheel-coiling in Bronze Age Crete. The Old Potter's Almanack 16 (2), 9–12.
Berg, I., Ambers, J., 2017. X-radiography of archaeological ceramics. In: Hunt, A.M.W. (Ed.), The Oxford Handbook of Archaeological Ceramic Analysis. Oxford University Press, Oxford, pp. 101–114.
Bernardini, F., Vecchiet, A., De Min, A., Lenaz, D., Mendoza Cuevas, A., Gianoncelli, A., Dreossi, D., Tuniz, C., 2016. Neolithic pottery from the trieste karst (northeastern Italy): a multi-analytical study. Microchem. J. 124, 600–607.
Bernardini, F., Tuniz, C., Zanini, F., 2019a. X-ray computed microtomography for paleoanthropology, archaeology, and cultural heritage. In: Lazzara, G., Fakhrullin, R. (Eds.), Advanced Nanomaterials, Nanotechnologies and Nanomaterials for Diagnostic, Conservation and Restoration of Cultural Heritage. Elsevier, pp. 25–45.
Bernardini, F., Leghissa, E., Prokop, D., Velušček, A., De Min, A., Dreossi, D., Donato, S., Tuniz, C., Princivalle, F., Montagnari Kokelj, M., 2019b. X-ray computed microtomography of Late Copper Age decorated bowls with cross-shaped foots from central Slovenia and the Trieste Karst (North-Eastern Italy): technology and paste characterisation. Archaeol. Anthropol. Sci. 11, 4711–4728. https://doi.org/10.1007/s12520-019-00811-w.
Bernardini, F., Vinci, G., Prokop, D., et al., 2020. A multi-analytical study of Bronze Age pottery from the UNESCO site of Al-Khutm (Bat, Oman). Archaeol Anthropol Sci 12, 163. https://doi.org/10.1007/s12520-020-01099-x.
Betancourt, P., 1979. Vasilike Ware. An Early Bronze Age Pottery Style in Crete. In: Studies in Mediterranean Archaeology, 56. P. Åströms, Göteborg.
Caloi, I., 2011. Le innovazioni tecnologiche nella Messarà: dal wheel-fashioning al wheel-throwing. In: Carinci, F., Cucuzza, N., Militello, P., Palio, O. (Eds.), ΚΡΗΤΗΣ ΜΙΝΩΙΔΟΣ. *Tradizione e identità minoica tra produzione artigianale, pratiche cerimoniali e memoria del passato* (Studi di Archeologia Cretese 10) Padova, pp. 87–102.
Caloi, I., 2012. Memory of a feasting event in the First Palace of Phaistos: preliminary observations on the bench deposit of Room IL. CretAnt 13, 41–59.
Caloi, I., 2019. Breaking with tradition? The adoption of the wheel-throwing technique at Protopalatial Phaistos: combining macroscopic analysis, experimental archaeology and contextual information. ASAtene 97, 9–25.
Caloi, I., 2021. Identifying wheel-thrown vases in Middle Minoan Crete? Preliminary Analysis of Experimental Replicas of Plain Handleless Conical Cups from Protopalatial Phaistos. Intedisciplinaria Archaeol XII, 201–216.
Choleva, M., 2012. The First Wheelmade pottery at Lerna: wheel-thrown or wheel-fashioned? Hesperia 81, 343–381.
Coleman, M.N., Colbert, M.W., 2007. Technical note: CT thresholding protocols for taking measurements on three-dimensional models. Am. J. Phys. Anthropol. 133, 723–725.
Courty, M.-A., Roux, V., 1995. Identification of wheel-throwing on the basis of ceramic surface features and microfabrics. J. Archaeol. Sci. 22, 17–50.
Day, P.M., Relaki, M., Faber, E.W., 2006. Pottery making and social reproduction in the bronze Age mesara. In: Wiener, M., Warner, J.L., Polonsky, J., Hayes, E. (Eds.), Pottery and Society: the Impact of Recent Studies in Minoan Pottery. Archaeological Institute of America, Boston, pp. 22–72.
Dean, M.C., Wood, B., 2003. A digital radiographic atlas of great apes skull and dentition. In: Bondioli, L., Macchiarelli, R. (Eds.), Digital Archives of Human Paleobiology. ADS Solutions, Milan (CD-ROM).
Di Vincenzo, F., Profico, A., Bernardini, F., Cerroni, V., Dreossi, D., Schlager, S., Zaio, P., Benazzi, S., Biddittu, I., Rubini, M., Tuniz, C., Manzi, G., 2017. Digital reappraisal and retrodeformation of the fossil human calvarium from Ceprano, Italy. Sci. Rep. 7, 13974.
Doherty, S.K., 2015. The Origins and Use of the Potter's Wheel in Ancient Egypt. Archaeopress, Oxford.
Doherty, S.K., 2021. The introduction of the potter's wheel to ancient Sudan. Interdisciplinaria Archaeol XII, 288–309.
Evely, R.D.G., 1988. The potters' wheel in Minoan Crete. BSA 83, 83–126.
Evely, R.D.G., 2000. Minoan crafts: tools and techniques. An introduction. P. Åströms, Jonsered.
Evely, R.D.G., Morrison, J.E., 2010. The Minoan potter's wheel: a study in experimental archaeology. In: Matthiae, P., Pinnock, F., Nigro, L., Marchetti, N. (Eds.), Proceedings of the 6th International Congress on the Archeology of the Ancient Near East, vol. I, pp. 283–288. Wiesbaden.
Fajardo, R.J., Ryan, T.M., Kappelman, J., 2002. Assessing the accuracy of high resolution X-ray computed tomography of primate trabecular bone by comparisons with histological sections. Am. J. Phys. Anthropol. 118, 1–10.
Gait, J., Bajnok, K., Szilágyi, V., et al., 2022. Quantitative 3D orientation analysis of particles and voids to differentiate hand-built pottery forming techniques using X-ray microtomography and neutron tomography. Archaeol Anthropol Sci 14, 223. https://doi.org/10.1007/s12520-022-01688-y.
Jeffra, C., 2013. A reexamination of early wheel potting in Crete. BSA 108, 31–49.
Kahl, W.A., Ramminger, B., 2012. Non-destructive fabric analysis of prehistoric pottery using high-resolution X-ray microtomography: a pilot study on the late Mesolithic to Neolithic site Hamburg-Boberg. JAS 39, 2206–2219. https://doi.org/10.1016/j.jas.2012.02.029.
Kozatsas, J., Kotsakis, K., Sagris, D., David, K., 2018. Inside out: assessing pottery forming techniques with micro-CT scanning. An example from Middle Neolithic Thessaly. J. Archaeol. Sci. 100, 102–119. https://doi.org/10.1016/j.jas.2018.10.007.
Knappett, C., 1999. Tradition and innovation in pottery forming technology: wheel-throwing at Middle Minoan Knossòs. BSA 94, 101–129.
Mentesana, et al., 2016. Looking for the invisible: landscape change and ceramic manufacture during the final neolithic-early bronze Age at Phaistos. In: Ghilardi, M. (Ed.), Géoarchéologie des iles de Méditérranée. CNR Éditions, Paris, pp. 299–310.
Rice, P.M., 1987. Pottery Analysis: A Source Book. University of Chicago Press, Chicago.
Roux, V., 2017. Ceramic manufacture: the chaîne opératoire approach. In: Hunt, A.M.W. (Ed.), The Oxford Handbook of Archaeological Ceramic Analysis. Oxford University Press, Oxford, pp. 101–114.
Roux, V., 2019. Ceramics and Society: a Technological Approach to Archaeological Assemblages. Springer, Cham.

Roux, V., Courty, M.-A., 1998. Identification of wheel-fashioning methods: technological analysis of 4th -3rd millennium BC Oriental ceramics. J. Archaeol. Sci. 25, 747–763.
Rye, O.S., 1977. Pottery manufacturing techniques: X-ray studies. Archaeometry 19, 205–211.
Rye, O.S., 1981. Pottery Technology: Principles and Reconstruction. Taraxacum.
Sanger, M., Thostenson, J., Hill, M., Cain, H., 2013. Fibrous twists and turns: early ceramic technology revealed through computed tomography. Appl. Phys. Mater. Sci. Process 111, 829–839. https://doi.org/10.1007/s00339-012-7287-6.
Sanger, M.C., 2016. Investigating pottery vessel manufacturing techniques using radiographic imaging and computed tomography: studies from the Late Archaic American Southeast. J. Archaeol. Sci. Rep. 9, 586–598. https://doi.org/10.1016/j.jasrep.2016.08.005.
Takenouchi, K., Yamahana, K., 2021. Fine pottery shaping techniques in Predynastic Egypt: a pilot study onnon-destructive analysis using an X-Ray CT scanning system. J. Archaeol. Sci. Rep 37 (11). https://doi.org/10.1016/j.jasrep.2021.102989.
Thér, R., 2020. Ceramic technology. How to reconstruct and describe pottery-forming practices. Archaeol. Anthropol. Sci. 12, 172. https://doi.org/10.1007/s12520-020-01131-0.
Thér, R., Mangel, T., 2024. Introduction of the potter's wheel as a reflection of social and economic changes during the La Tène period in Central Europe. Archaeol Anthropol Sci 16, 1. https://doi.org/10.1007/s12520-023-01890-6.
Thér, R., Wilczek, J., 2022. Identifying the contribution of rotational movement in pottery forming based on statistical surface analysis. Archaeol. Anthropol. Sci. 12 (14), 98.
Todaro, S., 2009. Pottery production in the Prepalatial Mesara: the Artisans' quarter to the West of the palace at Phaistos. CretAnt 10 (2), 333–352.
Todaro, S., 2016. Shaping tools and finished products from a pottery production area at Phaistos. A combined approach to the study of forming techniques in Early and Middle Minoan Crete. CretAnt 17, 273–325.
Todaro, S., 2018. What is essential is invisible to the eye. Multi-layered and internally supported vases at Protopalatial Phaistos. In: Baldacci, G., Caloi, I. (Eds.), Rhadamanthys. Studi di archeologia minoica in onore di Filippo Carinci per il suo 70° compleanno (BAR IS 2884). Oxford University Press, Oxford, pp. 39–48.
Tuniz, C., Bernardini, F., Turk, I., Dimkaroski, L., Mancini, L., Dreossi, D., 2012. Did Neanderthals play music? X-ray computed micro-tomography of the divje babe 'flute'. Archaeometry 54, 581–590.
Tuniz, C., Bernardini, F., Cicuttin, A., Crespo, M.L., Dreossi, D., Gianoncelli, A., Mancini, L., Mendoza Cuevas, A., Sodini, N., Tromba, G., Zanini, F., Zanolli, C., 2013. The ICTP-Elettra X-ray laboratory for cultural heritage and archaeology. Nucl. Instrum. Methods Phys. Res., Sect. A (711), 106–110.
Tuniz, C., Zanini, F., 2014. Microcomputerized tomography (MicroCT) in archaeology. In: Smith, C. (Ed.), Encyclopedia of Global Archaeology. Springer, New York, NY. https://doi.org/10.1007/978-1-4419-0465-2_675.
Van der Leeuw, S.E., 1976. Studies in the Technology of Ancient Pottery. University of Amsterdam, Amsterdam.
Zanolli, C., Martinón-Torres, M., Bernardini, F., Boschian, G., Coppa, A., Dreossi, D., et al., 2018. The Middle Pleistocene (MIS 12) human dental remains from Fontana Ranuccio (Latium) and Visogliano (Friuli-Venezia Giulia), Italy. A comparative high resolution endostructural assessment. PLoS One 1310, e0189773.